Charge-exchange scattering to the isobaric analog state at medium energies as a probe of the neutron skin

Bui Minh Loc,[1,2] Dao T. Khoa,[1] and R. G. T. Zegers[3]

[1]*Institute for Nuclear Science and Technology, VINATOM 179 Hoang Quoc Viet Rd., Hanoi, Vietnam*
[2]*University of Pedagogy, Ho Chi Minh City, Vietnam*
[3]*National Superconducting Cyclotron Laboratory and Department of Physics and Astronomy,*
Michigan State University, East Lansing, Michigan 48824-1321, USA

The charge-exchange (^{3}He,t) scattering to the isobaric analog state (IAS) of the target can be considered as "elastic" scattering of ^{3}He by the isovector term of the optical potential (OP) that flips the projectile isospin. Therefore, the accurately measured charge-exchange scattering cross section for the IAS can be a good probe of the isospin dependence of the OP, which is determined exclusively within the folding model by the difference between the neutron and proton densities and isospin dependence of the nucleon-nucleon interaction. Given the neutron skin of the target related directly to the same density difference, it can be well probed in the analysis of the charge-exchange (^{3}He,t) reactions at medium energies when the two-step processes can be neglected and the t-matrix interaction can be used in the folding calculation. For this purpose, the data of the (^{3}He,t) scattering to the IAS of ^{90}Zr and ^{208}Pb targets at $E_{\text{lab}} = 420$ MeV have been analyzed in the distorted wave Born approximation using the double-folded charge-exchange form factor. The neutron skin deduced for these two nuclei turned out to be in a good agreement with the existing database.

I. INTRODUCTION

The neutron skin thickness determined as the difference between the neutron and proton (root mean square) radii,

$$\Delta R_{np} = \langle r_n^2 \rangle^{1/2} - \langle r_p^2 \rangle^{1/2}, \tag{1}$$

was found by numerous structure studies to be strongly correlated with the slope of the symmetry energy of nuclear matter, i.e., the density dependence of the symmetry energy [1,2], which in turn is a key quantity for the determination of the equation of state of the neutron-rich nuclear matter. As a result, an accurate determination of the neutron skin has become an important research object of different nuclear reaction and structure studies (see a more detailed overview in Ref. [2]).

Although it is straightforward that we need to choose a well-defined and closely related to the neutron skin quantity that can be measured with high precision, the sensitivity of such experimental data to the neutron skin is often indirect and model dependent. Usually, a correlation between the neutron skin and such an experimental quantity is carefully investigated in some structure model using a realistic choice of the effective nucleon-nucleon (NN) interaction, and a conclusion on the neutron skin of the considered nucleus is then drawn. A recent example is the study of the electric dipole polarizability α_D of ^{208}Pb [3] based on both the microscopic random phase approximation approach and macroscopic droplet model, which gives $\Delta R_{np} \approx 0.165$ fm (with a total uncertainty around 25%) for this nucleus. Another famous attempt is the lead radius experiment (PREX) at the Thomas Jefferson National Accelerator Facility [4], where researchers measured the parity-violating electron scattering on the ^{208}Pb target and deduced in a rather model-independent way the neutron radius based on a larger weak charge of the neutron compared to that

of the proton. As a result, the PREX data suggested a neutron skin $\Delta R_{np} \approx 0.33^{+0.16}_{-0.18}$ fm for ^{208}Pb.

It is clear from Eq. (1) that the neutron skin is directly related to the difference between the neutron and proton densities, $\rho_n - \rho_p$, which is also known as the nuclear isovector (IV) density. The charge-exchange reactions (p,n) or (^{3}He,t) are the well-known probes of different IV excitations, such as the isobaric analog state (IAS), Gamow-Teller states, and spin-dipole resonances. The IAS of the ($Z + 1, N - 1$) nucleus has the same structure as the ground state (g.s.) of the (Z, N) target except for the replacement of a neutron by a proton, and its excitation energy is, therefore, almost equal to the Coulomb energy of the added proton. The two IASs are members of an isospin multiplet which have similar structures and differ only in the orientation of the isospin $\boldsymbol{T}$. Therefore, the (p,n) or (^{3}He,t) reaction to the IAS can be approximately considered as an "elastic" scattering process, with the isospin of the incident proton or ^{3}He being flipped [5–7]. In such a picture, the charge-exchange isospin-flip scattering to the IAS is naturally caused by the IV part of the optical potential (OP), expressed in the following Lane form [8]:

$$U(R) = U_0(R) + 4U_1(R)\frac{\boldsymbol{t}\boldsymbol{T}}{aA}. \tag{2}$$

Here $t = 1/2$ is the isospin of the projectile and T is that of the target with mass number A, R is the radial separation between the projectile and target, and $a = 1$ and 3 for the incident proton and ^{3}He, respectively. The second term of Eq. (2) is the *symmetry term* of the OP, with U_1 known as the Lane potential that contributes to both the elastic scattering and charge-exchange scattering to the IAS [7]. The empirical IV term of the proton-nucleus or ^{3}He-nucleus OP in the Woods-Saxon form was first used by Satchler *et al.* [5,6] as the charge-exchange form factor (FF) to describe the (p,n) or

(^{3}He,t) scattering to the IAS within the distorted wave Born approximation (DWBA).

In the standard isospin representation [9], the target nucleus A and *isobaric analog nucleus* $\tilde{A}$ can be referred to as the isospin states with $T_z = (N - Z)/2$ and $\tilde{T}_z = T_z - 1$, respectively. If we denote the state formed by adding proton or ^{3}He to A as $|aA\rangle$ and that formed by adding a neutron or triton to $\tilde{A}$ as $|\tilde{a}\tilde{A}\rangle$, then the DWBA charge-exchange FF for the (p,n) or (^{3}He,t) scattering to the IAS is readily obtained [9] from the transition matrix element of the OP (2) as

$$F_{\mathrm{cx}}(R) = \langle \tilde{a}\tilde{A}|4U_1(R)\frac{\boldsymbol{t}\boldsymbol{T}}{aA}|aA\rangle = \frac{2}{aA}\sqrt{2T_z}U_1(R). \quad (3)$$

The nucleon OP has been studied over the years, with several global sets of the OP parameters established from the extensive optical model (OM) analyses of the elastic nucleon scattering. Because the high-precision (p,n) data are not available for a wide range of target masses and proton energies, the IV term of the nucleon OP has been deduced [10–12] mainly from the OM studies of the elastic proton and neutron scattering from the same target and energy, where the IV term of the OP (2) has the same strength, but opposite signs for proton and neutron. Only in a few cases has the Lane potential U_1 been deduced from the DWBA studies of (p,n) scattering to the IAS [13,14]. With the Coulomb correction properly taken into account [15], the phenomenological Lane potential has been shown to account quite well for the (p,n) scattering to the IAS. However, a direct connection of the OP to the nuclear density can be revealed only when the OP is obtained microscopically from the folding model calculation [16–19].

The isospin dependence of the ^{3}He-nucleus OP has been less investigated. Moreover, the recent *global* OP for ^{3}He and triton [20] accounts fairly well for the elastic scattering data using a purely *isoscalar* real OP (with a slight dependence of the imaginary OP on the neutron-proton asymmetry). Therefore, one can learn more about the IV part of the ^{3}He-nucleus OP only in the study of the charge-exchange (^{3}He,t) reactions. In fact, the (^{3}He,t) scattering to the IAS has been studied in the DWBA with the FF obtained from a single-folding calculation, using the effective (isospin-dependent) ^{3}He-nucleon interaction and microscopic nuclear transition density for the IAS excitation [21,22].

II. ANALYSIS

The present work is our attempt to study the (^{3}He,t) scattering to the IAS based on Satchler's prescription (3). Thus, the FF of the (^{3}He,t) scattering to the IAS can be obtained from the double-folding model (DFM) [18,19] in the following compact form:

$$F_{\mathrm{cx}}(R) = \sqrt{\frac{2}{T_z}} \iint \big[\Delta\rho_1(\boldsymbol{r}_1)\Delta\rho_2(\boldsymbol{r}_2)v_{01}^{\mathrm{D}}(E,s)$$
$$+ \Delta\rho_1(\boldsymbol{r}_1,\boldsymbol{r}_1 + s)\Delta\rho_2(\boldsymbol{r}_2,\boldsymbol{r}_2 - s)$$
$$\times v_{01}^{\mathrm{EX}}(E,s)j_0(k(E,R)s/M)\big]d^3r_1\,d^3r_2, \quad (4)$$

where v_{01}^{D} and v_{01}^{EX} are the direct and exchange parts of the isospin-dependent term of the central NN interaction;

$\Delta\rho_i(\boldsymbol{r},\boldsymbol{r}') = \rho_n^{(i)}(\boldsymbol{r},\boldsymbol{r}') - \rho_p^{(i)}(\boldsymbol{r},\boldsymbol{r}')$ is the IV density matrix of the ith nucleus, which gives the local IV density when $\boldsymbol{r} = \boldsymbol{r}'$; $s = \boldsymbol{r}_2 - \boldsymbol{r}_1 + \boldsymbol{R}$, and $M = aA/(a + A)$. The relative-motion momentum $k(E,R)$ is given self-consistently by the real OP at the distance R (see details in Refs. [18,19]). In the limit $a \to 1$ and $\Delta\rho_1 \to 1$, the integration over $\boldsymbol{r}_1$ disappears and Eq. (4) is reduced to a single-folded expression for the FF of the (p,n) scattering to the IAS [19]. Because the energies of the analog states are separated approximately by the Coulomb displacement energy, the charge-exchange scattering to the IAS has a nonzero Q value. To account for this effect, the double-folded FF (4) is evaluated at the energy of $E = E_{\mathrm{lab}} - Q/2$, midway between the energies of the incident ^{3}He and emergent triton, as suggested by Satchler *et al.* [6].

At the incident energies of 100∼200 MeV/nucleon the impulse approximation is reasonable, and an appropriate t-matrix parametrization of the free NN interaction can be used in Eq. (4). Following the DWBA analysis of the (^{3}He,t) reaction at the same energy to study the Gamow-Teller excitations [23,24], we have used in the present work the nonrelativistic t-matrix interaction suggested by Franey and Love [25,26] based on the experimental NN phase shifts. Thus, the isospin-dependent direct and exchange parts of the central NN interaction are determined from the singlet and triplet even (SE,TE) and odd (SO,TO) components of the local t-matrix interaction [26] as

$$v_{01}^{\mathrm{D(EX)}}(s) = \frac{k_a k_A}{16}[-3t_{\mathrm{TE}}(s) + t_{\mathrm{SE}}(s) \pm 3t_{\mathrm{TO}}(s) \mp t_{\mathrm{SO}}(s)]. \quad (5)$$

Here k_a and k_A are the energy-dependent kinematic modification factors of the t-matrix transformation from the NN frame to the Na and NA frames, respectively, which are given by Eq. (19) of Ref. [25]. The explicit (complex) strength of the *finite-range* t-matrix interaction (5) is given in terms of four Yukawa functions [26]. We note also that at medium energies, the two-step processes like (^{3}He,α)(α,t) or (^{3}He,d)(d,t) are negligible and the direct charge-exchange process is dominant, which allows one to deduce accurately the strength of the Fermi or Gamow-Teller transitions [23,24].

Another important nuclear structure input to the folding integral (4) are the neutron and proton g.s. densities of the ^{3}He projectile and target nucleus. In the present work, we have used the neutron and proton densities of ^{3}He given by the microscopic three-body calculation [27] using the Argonne NN potential. For the ^{90}Zr and ^{208}Pb targets we have used the empirical neutron and proton densities deduced from the high-precision elastic proton scattering at 800 MeV by Ray *et al.* [28,29]. These densities are given in the analytic form so that one can slightly adjust the radial parameter of the neutron density to the best DFM + DWBA description of the charge-exchange (^{3}He,t) scattering data under study, and determine the corresponding neutron skin. For the comparison, we have also used the microscopic nuclear g.s. densities given by the Hartree-Fock-Bogoliubov (HFB) calculation [30] using the realistic Skyrme interaction and taking into account the continuum. These HFB densities have been used earlier in the folding model analysis [31] to study the total reaction cross sections measured at medium energies for the unstable nuclei.

The differential cross section of the charge-exchange Fermi transition to the IAS, with $\Delta L = \Delta S = 0$, and $\Delta T = 1$, is known to peak at the zero scattering angle. The absolute differential cross sections measured at the forward scattering angles ($\theta_{\text{lab}} = 0°{-}2.5°$) for the ^{90}Zr,^{208}Pb(^{3}He,t) reactions to the IAS were available from a previous study [23], performed at the Grand Raiden Spectrometer at the Research Center for Nuclear Physics in Osaka. The ^{3}He beam energy was 420 MeV. Further details of the experiment can be found in Ref. [23] and references therein. The uncertainty in the extracted absolute differential cross sections was about 10% and predominantly related to the uncertainty in the current integration of the unreacted beam in a Faraday cup. The ^{90}Zr and ^{208}Pb targets were isotopically pure ($>$99%).

For the DWBA analysis of the considered charge-exchange reactions, an accurate determination of the distorted waves in the entrance and exit channels by the appropriately chosen OP is very crucial. Although it is tempting to use consistently the total OP (2) given by the double-folding calculation using the same t-matrix interaction, such an attempt results in a poorer description of both the elastic scattering and charge-exchange data. A plausible reason is that the higher-order medium corrections to the microscopic OP are not negligible at the considered energy. Therefore, we have used in the present DWBA analysis the phenomenological OP of the ^{3}He + ^{90}Zr system taken from Ref. [32]. The complex OP of the ^{3}He + ^{208}Pb system has been obtained from a new OM fit [23] of the elastic ^{3}He scattering data at 450 MeV [33], with the relativistic kinematics. Following the earlier DWBA studies of the (^{3}He,t) reactions [21–24], the ^{3}He OP rescaled by a factor $k = 0.85$ has been used for the triton OP of the exit channel. All the DWBA calculations of the charge-exchange scattering to the IAS were done with the relativistic kinematics, using the code ECIS97 written by Raynal [34].

III. RESULTS

The results of our DFM + DWBA analysis of the (^{3}He,t) scattering to the IAS of the ^{90}Zr target are shown in Fig. 1. Among the inputs of the folding calculation of the charge-exchange FF (4), only the radial parameter of the empirical neutron density by Ray *et al.* [28] is slightly adjusted to obtain the best DWBA fit to the charge-exchange data. Such a simple linear fit results on a neutron density that gives the neutron skin $\Delta R_{np} \approx 0.09 \pm 0.03$ fm. The uncertainty of the (best-fit) neutron skin is associated with the experimental uncertainty around 10% of the absolute differential cross section measured at the most forward angles. The obtained best-fit neutron skin is rather close to that given by the microscopic HFB density ($\Delta R_{np} = 0.07$ fm) [30]. If the charge-exchange FF (4) is calculated using the HFB density, then the DWBA results agree reasonably (within the error band) with those given by the (modified) empirical density. It is worth noting that the (p,n) data of the spin-dipole excitations of the ^{90}Zr target have been analyzed [35] to deduce accurately the spin-dipole sum rule strength that gives the neutron skin $\Delta R_{np} \approx 0.07 \pm 0.04$ fm for this nucleus, about the same as that given by the HFB calculation. The best-fit neutron skin of ^{90}Zr given by the present DFM + DWBA analysis is close to that
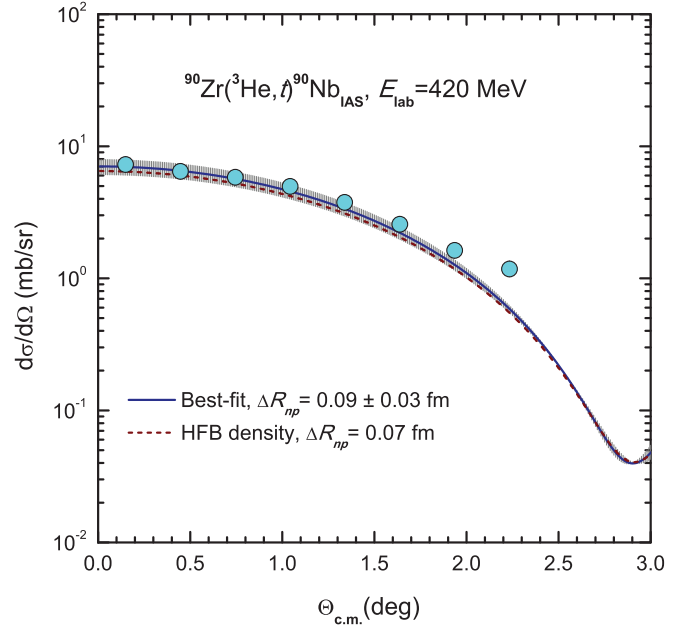

FIG. 1. (Color online) DWBA description of the (^{3}He,t) scattering to the IAS of the ^{90}Zr target given by the charge-exchange FF (4) based on the empirical IV density by Ray *et al.* [28], adjusted by the best DWBA fit to the data. The error of the (best-fit) neutron skin was determined to account for the experimental uncertainty around 10% of the absolute differential cross section measured at the most forward angles (the hatched area). The dashed curve is the prediction given by the microscopic HFB density [30].

($\Delta R_{np} \approx 0.085$ fm) given by the analysis of the elastic proton scattering data measured at $E_p = 800$ MeV with the ^{90}Zr target [28,29].

Given the indirect relation of the neutron skin of ^{208}Pb to the behavior of the nuclear symmetry energy, it has become a hot research topic recently [1–4,36,37]. Although the PREX data seem to provide for the first time an accurate, model-independent determination of the neutron skin of ^{208}Pb [4], the mean ΔR_{np} value deduced from the PREX data is significantly higher than that given by other studies [3,36], including the preliminary results of the γ-induced pion production [37]. The results of the DFM + DWBA analysis of the (^{3}He,t) scattering to the IAS of ^{208}Pb are shown in Fig. 2. After the radial parameter of the empirical neutron density taken from Ref. [28] was adjusted to the best DFM + DWBA fit to the ^{208}Pb(^{3}He,t)^{208}Bi$_{\text{IAS}}$ data, a neutron skin $\Delta R_{np} \approx 0.16 \pm 0.04$ fm was obtained for ^{208}Pb. As in the ^{90}Zr case, the uncertainty of the best-fit ΔR_{np} value resulted from the experimental uncertainty of about 10% in the normalization of the absolute differential cross section measured at the forward angles. Although the error bars of the best-fit neutron skin might be larger due to the uncertainty of the choice of the OP for the entrance and exit channels, the ΔR_{np} value obtained in our DFM + DWBA analysis is in good agreement with that reported by other structure studies [2,3,36,37]. It is interesting to note that the use of the microscopic HFB density [30] in the DFM calculation (with the associated $\Delta R_{np} = 0.17$ fm)
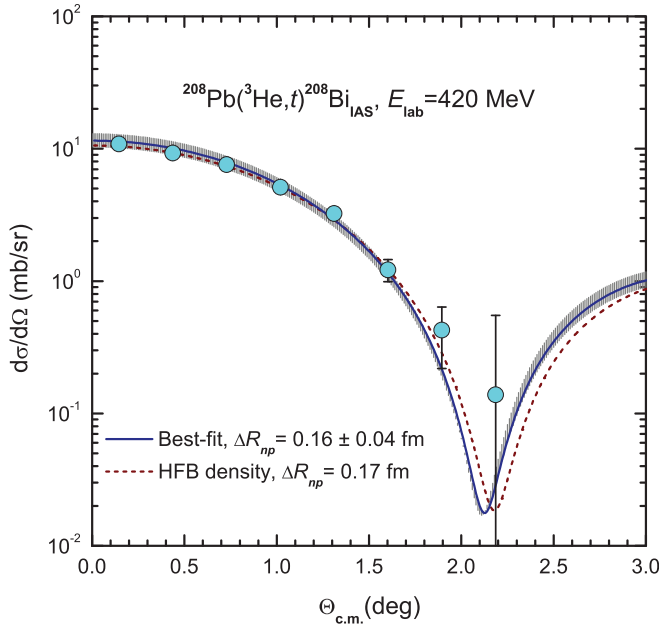
FIG. 2. (Color online) Same as Fig. 1, but for the ^{208}Pb target.

results in a very good overall agreement of the DWBA result with the ^{208}Pb(^{3}He,t)^{208}Bi$_{\text{IAS}}$ data (see dashed curve in Fig. 2).

For a comparison, we have made further a DFM + DWBA calculation using the IV nuclear density of ^{208}Pb constructed to give the same neutron skin as that given by the PREX data. From these results (see Fig. 3) one can see that the lower edge of the PREX data agrees nicely with the measured (^{3}He,t) data. Consequently, we still cannot rule out the large neutron skin of
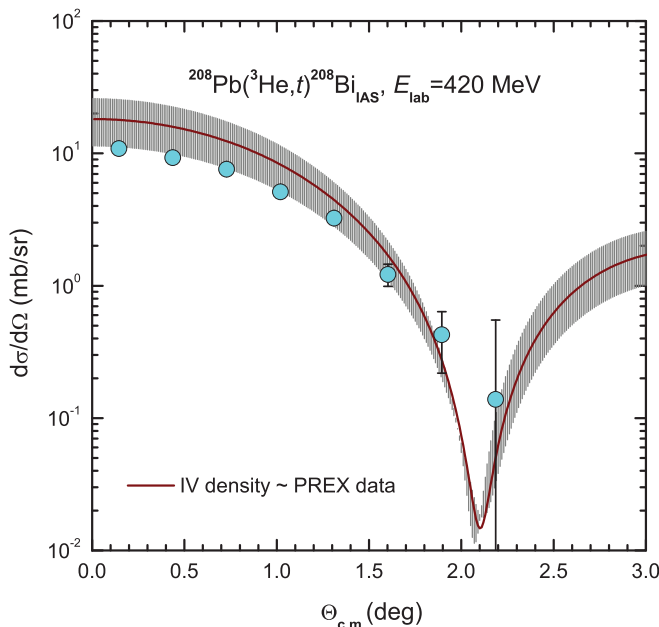

FIG. 3. (Color online) DWBA description of the (^{3}He,t) scattering to the IAS of the ^{208}Pb target given by the charge-exchange FF (4) based on the empirical IV density by Ray *et al.* [28], adjusted to reproduce the PREX data for the neutron skin, $\Delta R_{np} \approx 0.33^{+0.16}_{-0.18}$ fm [4].
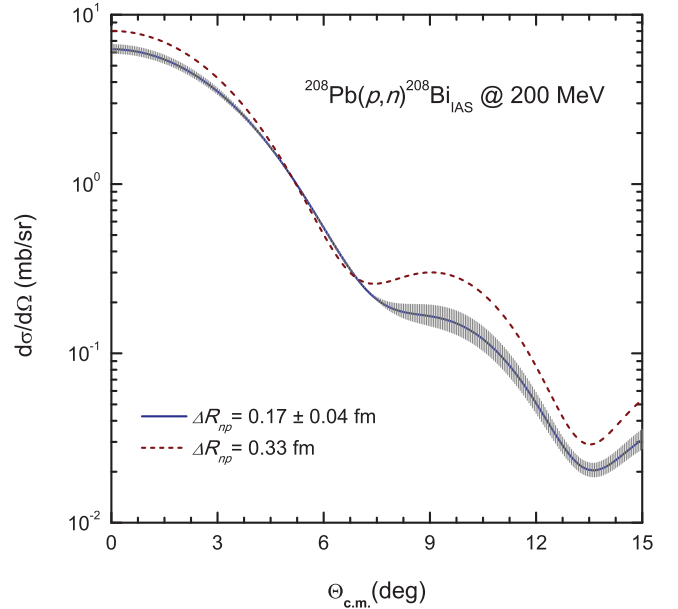

FIG. 4. (Color online) DWBA prediction of the (p,n) scattering to the IAS of the ^{208}Pb target at $E_p = 200$ MeV given by the folded FF based on the empirical IV density by Ray *et al.* [28], adjusted to reproduce the best-fit neutron skin of ^{208}Pb given by the present DFM + DWBA analysis of the (^{3}He,t) data and the mean ΔR_{np} value given by the PREX data [4].

^{208}Pb given by the PREX measurement, as was also concluded recently by Fattoyev and Piekarewicz [36]. The new PREX experiment planned to pin down the uncertainty of the ΔR_{np} value to about 0.06 fm [1] would surely resolve the uncertainty of the DFM + DWBA results shown in Fig. 3.

Despite numerous elastic proton scattering data taken at medium energies, the high-precision data of the (p,n) scattering to the IAS at medium energies are still not available. We found it of interest to make a folding + DWBA prediction of the (p,n) scattering to the IAS of ^{208}Pb at the proton energy of 200 MeV. From the results shown in Fig. 4 one can see that the effect caused by different neutron skin values is significant not only at the zero scattering angle but also at the first diffraction maximum. With the modern neutron detection technique, it should be feasible to cover the whole oscillation pattern of the (p,n) scattering cross section at the forward region and, eventually, allow one to fine tune the neutron skin value in a similar folding + DWBA analysis.

IV. CONCLUSION

In conclusion, the existing data of the (^{3}He,t) scattering to the IAS of ^{90}Zr and ^{208}Pb at $E_{\text{lab}} = 420$ MeV have been studied in a detailed DFM + DWBA analysis to deduce the neutron skin values for these two nuclei. The best-fit neutron skin values given by our analysis are in a good agreement with those given by the recent nuclear structure studies.

[1] C. J. Horowitz, E. F. Brown, Y. Kim, W. G. Lynch, R. Michaels, A. Ono, J. Piekarewicz, M. B. Tsang, and H. H. Wolter, arXiv:1401.5839 [J. Phys. G (to be published)].

[2] M. B. Tsang *et al.*, Phys. Rev. C **86**, 015803 (2012).

[3] X. Roca-Maza, M. Brenna, G. Colò, M. Centelles, X. Viñas, B. K. Agrawal, N. Paar, D. Vretenar, and J. Piekarewicz, Phys. Rev. C **88**, 024316 (2013).

[4] S. Abrahamyan *et al.* (PREX Collaboration), Phys. Rev. Lett. **108**, 112502 (2012).

[5] R. M. Drisko, R. H. Bassel, and G. R. Satchler, Phys. Lett. **2**, 318 (1962).

[6] G. R. Satchler, R. M. Drisko, and R. H. Bassel, Phys. Rev. **136**, B637 (1964).

[7] G. R. Satchler, in *Isospin in Nuclear Physics*, edited by D. H. Wilkinson (North-Holland, Amsterdam, 1969), p. 390.

[8] A. M. Lane, Phys. Rev. Lett. **8**, 171 (1962).

[9] G. R. Satchler, *Direct Nuclear Reactions* (Clarendon Press, Oxford, 1983).

[10] F. D. Becheetti and G. W. Greenlees, Phys. Rev. **182**, 1190 (1969).

[11] R. L. Varner, W. J. Thompson, T. L. McAbee, E. J. Ludwig, and T. B. Clegg, Phys. Rep. **201**, 57 (1991).

[12] A. J. Koning and J. P. Delaroche, Nucl. Phys. A **713**, 231 (2003).

[13] J. D. Carlson, C. D. Zafiratos, and D. A. Lind, Nucl. Phys. A **249**, 29 (1975).

[14] G. C. Jon *et al.*, Phys. Rev. C **62**, 044609 (2000).

[15] R. P. DeVito, D. T. Khoa, S. M. Austin, U. E. P. Berg, and B. M. Loc, Phys. Rev. C **85**, 024619 (2012).

[16] D. T. Khoa, E. Khan, G. Colò, and N. V. Giai, Nucl. Phys. A **706**, 61 (2002).

[17] D. T. Khoa, H. S. Than, and D. C. Cuong, Phys. Rev. C **76**, 014603 (2007).

[18] D. T. Khoa, W. von Oertzen, and A. A. Ogloblin, Nucl. Phys. A **602**, 98 (1996).

[19] D. T. Khoa, B. M. Loc, and D. N. Thang, Eur. Phys. J. A **50**, 34 (2014).

[20] D. Y. Pang, P. Roussel-Chomaz, H. Savajols, R. L. Varner, and R. Wolski, Phys. Rev. C **79**, 024615 (2009).

[21] S. Y. van Der Werf, S. Brandenburg, P. Grasduk, W. A. Sterrenburg, M. N. Harakeh, M. B. Greenfield, B. A. Brown, and M. Fujiwara, Nucl. Phys. A **496**, 305 (1989).

[22] J. Jänecke *et al.*, Nucl. Phys. A **526**, 1 (1991).

[23] R. G. T. Zegers *et al.*, Phys. Rev. Lett. **99**, 202501 (2007).

[24] G. Perdikakis *et al.*, Phys. Rev. C **83**, 054614 (2011).

[25] W. G. Love and M. A. Franey, Phys. Rev. C **24**, 1073 (1981).

[26] M. A. Franey and W. G. Love, Phys. Rev. C **31**, 488 (1985).

[27] E. Nielsen, D. V. Fedorov, A. S. Jensen, and E. Garrido, Phys. Rep. **347**, 373 (2001).

[28] L. Ray, G. W. Hoffmann, G. S. Blanpied, W. R. Coker, and R. P. Liljestrand, Phys. Rev. C **18**, 1756 (1978).

[29] L. Ray, W. R. Coker, and G. W. Hoffmann, Phys. Rev. C **18**, 2641 (1978).

[30] M. Grasso, N. Sandulescu, N. Van Giai, and R. J. Liotta, Phys. Rev. C **64**, 064321 (2001).

[31] D. T. Khoa, H. S. Than, T. H. Nam, M. Grasso, and N. V. Giai, Phys. Rev. C **69**, 044605 (2004).

[32] J. Kamiya *et al.*, Phys. Rev. C **67**, 064612 (2003)

[33] T. Yamagata, H. Utsunomiya, M. Tanaka, S. Nakayama, N. Koori, A. Tamii, Y. Fujita, K. Katori, M. Inoue, M. Fujiwara, and H. Ogata, Nucl. Phys. A **589**, 425 (1995).

[34] J. Raynal, *Computing as a Language of Physics* (IAEA, Vienna, 1972), p. 75; coupled-channel code ECIS97 (unpublished).

[35] K. Yako, H. Sagawa, and H. Sakai, Phys. Rev. C **74**, 051303(R) (2006).

[36] F. J. Fattoyev and J. Piekarewicz, Phys. Rev. Lett. **111**, 162501 (2013).

[37] C. M. Tarbert *et al.*, arXiv:1311.0168.